Iranian Journal of Geophysics, Vol 15 No 4, 2022, Page 101 – 114 (Research Article)
DOI: 10.30499/IJG.2021.289366.1333

Stochastic modeling of gravity data for 2D basement reliefs without regularization coefficient

Mahmoud Reshadati [1] and Seyed-Hani Motavalli-Anbaran [2*]

[1] *M.Sc Graduate Institute of Geophysics, University of Tehran, Tehran, Iran*
[2] *Assistant Professor, Institute of Geophysics, University of Tehran, Tehran, Iran*

(Received: 05 June 2021, Accepted: 07 August 2021)

Abstract

In this paper, a modified version of strength Pareto evolutionary algorithm SPEA (II) is used as a multi-objective optimization method in gravity data modelling. In this method, a two-dimensional gravity inversion problem is solved by iteratively random creation of forward models. It is shown that it can be used as a fast and effective inversion tool in the depth modelling of two-dimensional layer problems with applications in depth-to-basements, geometry of bedrocks and sedimentary basins modelling cases. Owing to the direct use of the regularization term as a separate objective function, smooth models have a high chance of being selected as final solutions, which makes the results more acceptable and easier to interpret. The most important advantages of this method are that it works independently of the regularization coefficient; thus, there is no need to run the algorithm so many times to find a proper regularization parameter. Furthermore, there is no need to directly deal with inverse formulations, and last but not least, by using a multi-objective algorithm as a global optimization method, convergence to a stable solution does not depend on the initial model, the way classical inversion methods do. For testing the algorithm, a synthetic model is used for layer boundary modelling and to assess the stability of this algorithm, white Gaussian noise is added to the synthetic model. To evaluate the validity of this method, real data from the Recôncavo basin in Brazil is considered for processing and inversion, and the results are compared to the ones from previous studies. All computations have been done in the GNU Octave 5.1.0 environment.

Keywords: Gravity, inversion, regularization coefficient, multi-objective, Genetic, basement relief

* Corresponding author: motavalli@ut.ac.ir

1 Introduction

Inversion of gravity data is generally defined as an ill-posed problem. A good inversion algorithm needs to guarantee that the suggested results are reasonable and stable, satisfying mathematical, geophysical and geological conditions simultaneously. The necessity for meeting all these conditions in one solution makes the solving process rather long and hard. Thus, different algorithms were proposed for either 2D or 3D inversion of gravity data with the aim of improving the geological validity of results and also, improving the different aspects of the inversion process such as complexity and time reduction. Among them, evolutionary algorithms, especially Genetic Algorithm (GA), are well known as global optimization methods. Lawrence and Phillips (2003) applied a niching genetic algorithm as an inversion tool for gravity/topography data. Zhang et al. (2004) used a parallel genetic algorithm for inversion of gravity data as a mean to investigate the crustal structure in central Taiwan. Montesinos et al. (2005) used the genetic algorithm for 3D modelling of gravity data for volcanic sources in the Canary Islands.

Multi-objective optimizations (Coello, 1999) are the emerging ones among global optimization methods which their applications are well established in applied geophysics. These methods are generally useful especially when inversion of different data types are required, in which using classical inversion techniques gets complicated due to a large number of parameters. Akca et al. (2014) inverted both magnetic resonance and vertical electric soundings with a multi-objective genetic algorithm and Miernik et al. (2016) used a Pareto based multi-objective method for inversion of 2D gravity and magneto-telluric data.

In most researches, Tikhonov objective function is used as a cost function for inversion of potential data. This function itself is a summation of two different terms: the data misfit (fidelity term) and the regularization function. A general approach is to augment a weighted regularization function to increase the stability of the inversion process. A suitable regularization function with a proper weight would reduce the model search space, decrease the time of the inversion process and shrink the non-unity of solution space. But finding a suitable regularization function and also estimation of appropriate weight itself has been an interesting topic for researches. For estimating the regularization coefficient (the trade-off between regularization term and data misfit term), different optimization methods are proposed such as Morozov discrepancy principle formulated by Morozov (1966) and generalized cross-validation by Golub et al. (1979). Hansen (1992) used the L-curve method in discrete ill-posed problems analysis, and Li and Oldenburg (1999) used it for inversion of geophysical data.

In this paper, we use a modified version of a multi-objective algorithm developed by Zitzler et al. (2001) as an inversion tool for our gravity data. SPEA II (Strength Pareto Evolutionary Algorithm II) is originated from the first version of SPEA (Zitzler and Thiele, 1999) with some technical developments that turn it into a completely effective algorithm. In general, multi-objective algorithms search for a solution set by simultaneously direct optimization of different function without using gradient information, the way Lagrangian method does. Better solutions are selected by the concept of domination and dominant solutions form a possibly acceptable solution subset called Pareto front. An evolutionary algorithm (which is GA here) is then used for the creation of another solution set derived from previously dominant solutions for the next iteration of the algorithm. This loop will be repeated for a preset number or when a specific condition is met.

We use this algorithm for inversion of 2D gravity data, specifically for modelling a 2D layer boundary with a predefined homogenous density contrast. Using gravity technique in layer boundary determination, especially for the case of sedimentary basins, is the most applicable method among potential exploration techniques. Other methods – magnetic or electric – may not provide enough information due to the lack of discernible susceptibility or resistivity contrast in the area, whereas in most cases there is a significant density contrast between sediments and bedrocks. For gravity modelling, we use two-dimensional Talwani method (Talwani et al. 1959) as a model generator in the optimization algorithm. For regularization strategy, we use a regularization term not in form of an augment to the data misfit term, but as a separate objective function. To achieve a more efficient algorithm, some important modifications are applied in genetic operations. Different synthetic models are tested in order to evaluate the stability and efficiency of the algorithm and the results are analyzed. As a practical application of this method, a profile of gravity data in the Recôncavo basin in Brazil is considered for inversion and the results are presented.

2 Research method

2-1 Multi-objective literature and structure

In this algorithm, our first aim is to search for the subsurface geometry of a 2D layer with a predefined homogenous density distribution under a profile of observed gravity data, so the parameters we are trying to determine in the models are the depth values. An array of depth parameters will be named a solution. A solution with its gravity output is called a model. A set of solutions is called a population. In the each iteration of the algorithm, a population is available for assessment. Typically, generally solutions that create a better gravity effect are preferred. A better gravity effect means a better fit to the observed data and to be in accordance with constraints defined by the operator or a-priori information.

The exact meaning of a better solution is defined by the concept of dominance, which will be described later in this paper. After the assessment of all solutions in a population, dominant solutions are saved in a finite space called archive. The solutions in the archive are the best solutions found in the algorithm and they will be used for generation of next possible solutions and creation of the next population. In the next iteration, the newly created solutions and the previous archive solutions will be compared and assessed again, and the better solutions will be rewritten in the archive. This cycle will continue to a finite iteration number or when a special condition met.

2-2 Forward modelling

To calculate the gravity effect of a solution, as it is shown in Fig. 1, the Talwani method is used as it is expressed by Telford et al. (1990):

$$\boldsymbol{G} = 2\boldsymbol{\gamma\rho}.\sum_{i=1}^{\boldsymbol{N}} \boldsymbol{a_i} \sin\emptyset_i . \cos\emptyset_i \left[(\theta_i - \theta_{i+1}) + \tan\emptyset_i . \log\left\{\frac{\cos\theta_i(\tan\theta_i - \tan\emptyset_i)}{\cos\theta_{i+1}(\tan\theta_{i+1} - \tan\emptyset_i)}\right\}\right] \quad (1)$$

where a_i is:

$$\boldsymbol{a_i} = (\boldsymbol{x_{i+1}} - \boldsymbol{z_{i+1}}.\cot\emptyset_i) \quad (2)$$

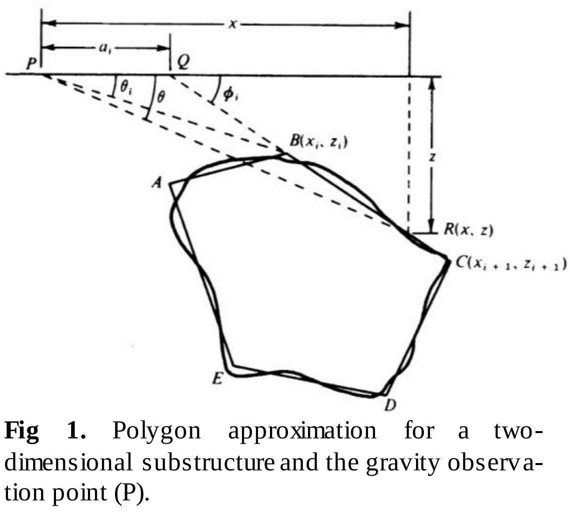

Fig 1. Polygon approximation for a two-dimensional substructure and the gravity observation point (P).

Here, ρ is the density contrast between the polygon and environment, γ is the gravitational constant and G is the vertical component of gravity effect from the two-dimensional polygon. The parameters θ_i and $\emptyset_i$ pertaining to node $\mathbf{i}$ are shown in Fig. 1. N is the number of nodes of the polygon. The goal is to determine the geometry of a layer confined by topography from the top, so for this case of study, the upper boundary of Talwani polygon is the topography and the lower boundary of the polygon is considered as the geometry of layer. This means the parameter space for a solution can be depicted as a (1×N) array. Talwani formula is based on the fact that by calculating a line integral around the perimeter of an n-sided polygon, one can compute the vertical component of the gravitational attraction of a 2D n-sided polygon (Hubert, 1948):

$$\boldsymbol{G} = 2\boldsymbol{\gamma}\boldsymbol{\rho}\int \boldsymbol{z}\boldsymbol{d}\boldsymbol{\theta}. \quad (3)$$

Thus, many different formulations of this integral are presented. Here a vectorized version of the main formula presented by Telford et al. (1990) is used to increase the efficiency of the code.

2-3 Initial set of solutions

For the first iteration of the multi-objective algorithm, we need a set of random depth models as candid solutions (initial population). These candid solutions will be used as starting points for further model creations and assessments. One of the main advantages of using global optimization methods over classical linear inversion techniques is that classical inversion methods heavily depend on the initial models while global optimization methods investigate the entire search space which makes the algorithm - in most cases - avoid local minima. However, this does not mean the algorithm will always end up in globally optimized solutions, especially when a proper coverage of search space is not available. Thus, sufficient diversity among initial models plays an important role in the exploration of search space in the next iterations, so using a large number of totally random initial models will be a good strategy.

2-4 Objective functions

For the inversion of gravity data in multi-objective functions, similar to the Tikhonov function, minimizing two objective functions are considered. One function is the fidelity term and the other is the constraints term, called regularization function. For a suggested model (**m**) with an array of depth values (**z**), the general form of fidelity term is the weighted $L2$ norm of errors:

$$\boldsymbol{f_1}(\boldsymbol{m}) = ||\boldsymbol{W}_d(\boldsymbol{Gm} - \boldsymbol{g}_{obs})||^2 \quad (4)$$

where the term $\boldsymbol{Gm}$ is the gravitational attraction of the suggested model (**m**), the $\boldsymbol{g}_{obs}$ is observed gravity and $\boldsymbol{W}_d$ is the weighting matrix of the observed data. In the multi-objective algorithm and for the case of 2D layer boundary determination, we compute RMSE for gravity misfit error of all observation points like i:

$$\boldsymbol{f_1}(\boldsymbol{m}) = \sqrt{\frac{1}{\boldsymbol{N}_{obs}}\sum_i(\boldsymbol{g}(\boldsymbol{m})_i^{cal} - \boldsymbol{g}_{\boldsymbol{i}}^{obs})^{\,2}} \quad (5)$$

The gravity effect of model (**m**), which is $(\boldsymbol{g}(\boldsymbol{m})_i^{cal})$ will be calculated from the Talwani forward method as mentioned above. For the other objective function (the regularization term), the second term of Tikhonov function is the initial suggestion:

$$\boldsymbol{f_2}(\boldsymbol{m}) = \lambda^2||\boldsymbol{W}_m(\boldsymbol{m} - \boldsymbol{m}_0)||^2 \quad (6)$$

where $\boldsymbol{W}_m$ is the weighting matrix of constrains, λ is the regularization parameter and $\boldsymbol{m}_0$ is an initial model suggested by the user. As we discussed in previous section, in global optimization methods, we run the algorithm independent to an initial model like $\boldsymbol{m}_0$. Furtheremore, by separate use of objective functions $\boldsymbol{f_1}(\boldsymbol{m})$ and $\boldsymbol{f_2}(\boldsymbol{m})$, and avoiding the summation, the regularization parameter λ will be eliminated. Consequently, the last formula will be shrunk to:

$$f_2(m) = ||W_m(m)||^2 \quad (7)$$

In this paper, the first norm of the model constrains in form of Mean Absolute Error (MAE) of depth values is used:

$$f_2(m) = \frac{1}{N_m}\sum_i|(\Delta m)| \quad (8)$$

2-5 Dominance and Pareto front

After creation of a set of random initial solutions (models), both objective functions will be computed for every single solution and these solutions are compared in objective function space (Fig. 2). A better solution would be defined as a dominating solution if two conditions are met:

- No solution is better than the dominant solution for all values of objective functions.
- The dominant solution has at least one better objective function value than the other solutions.

In this research, we aim to minimize both objective functions $f_1(m)$ and $f_2(m)$ for a model (**m**), so for two different models **m1** and **m2**, we have three different situations. First:

$$f_1(m1) > f_1(m2) \wedge f_2(m1) > f_2(m2) \quad (9)$$

In this circumstance, it is called that solution **m2** dominates solution **m1**. Second:

$$f_1(m1) < f_1(m2) \wedge f_2(m1) < f_2(m2) \quad (10)$$

In this situation, **m1** is the dominant solution and **m2** is the dominated solution. And finally:

(11)

$$f_1(m1) < f_1(m2) \wedge f_2(m1) > f_2(m2)$$

or

$$f_1(m1) > f_1(m2) \wedge f_2(m1) < f_2(m2)$$

In this condition, models do not dominate each other. It means no solution is better than the other one. As a result, both are valid models and will be considered for the next iteration. After checking the dominance condition for every possible pair of the models in the population, there will be some models that are not dominated at all. These solutions are called dominant solutions, forming the Pareto front (Coello, 1999). In Fig. 2, the solutions 1, 4 and 5 are in the Pareto front.

The next section (2-6) is fully covered in Zitzler et al. (2001). However, for a complete narration of the details applied in our code, there is a piece of concise information.

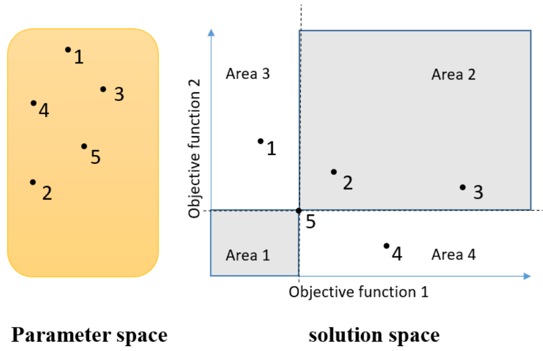

Fig 2. Mapping of solutions (models) between spaces. In parameter space, each model has an array of depth values, whereas in solution space, each model is identified by two objective function values. The dominance concept is defined in the solution space. In a minimization problem (like the case we seek in this research), model No. 5 dominates both model No. 2 and No. 3, while it cannot dominate models No. 1 and No. 4. Any possible models founded in area 1 would dominate model No. 5.

2-6 Strength Pareto concept

To completely numerate the fitness of a solution and to represent how good a solution is in comparison to other solutions, two factors are considered in the algorithm. The first one is how many times a solution m_i is dominated by other solutions. It is defined as:

$$R(m_i) = \sum_{j\in pop+archive,\ j\gg i} S(m_j) \quad (12)$$

where $S(m_j)$ represents the number of solutions that model m_j dominates in the solution space. The symbol ≅≫A is domination operation, so $(m_j \gg m_i)$ means model m_j dominates model m_i. Finally, $R(m_i)$ which is an integer number between [0 , ∞), is called raw fitness of solution m_i depicting the fact that how many times the model is dominated. Therefore, it can be easily understood that for a non-dominated solution, the raw fitness values is $R(m_i) = 0$.

The second factor is a parameter that describes how far a solution is from other solutions. The density function for model $\boldsymbol{m_i}$ is defined as:

$$\boldsymbol{D}(\boldsymbol{m_i}) = \frac{1}{\sigma_{m_i}^{k}+2};\ k = \sqrt{N_{pop} + N_{arch}} \qquad (13)$$

Here, $\boldsymbol{\sigma_i^k}$ which is the k-th nearest neighbor distance for model $\boldsymbol{m_i}$, is computed by using the k-th nearest neighbor method (Silverman, 1986). N_{pop} is population size and N_{arch} is archive size. We can see that the density function $\boldsymbol{D}(\boldsymbol{m_i})$ has a value between 0 and 0.5. The value 0 corresponds to an almost isolated model in the solution space. It is important to note that dispersed models are essential to be saved for further investigation of solution space.

Summation of raw fitness and density functions forms total fitness of a model:

$$\boldsymbol{F}(\boldsymbol{m_i}) = \boldsymbol{R}(\boldsymbol{m_i}) + \boldsymbol{D}(\boldsymbol{m_i}) \qquad (14)$$

Better solutions have lower total fitness value and will be added to archive. In case of which the population of archive became larger than a predefined maximum size, models with higher values of $\boldsymbol{F}$, would be removed.

2-7 GA general operators

New set of solutions is created by genetic operations. In genetic algorithm, models used for a new generation of solutions are called parents and newly generated models are the children. In this algorithm, arithmetic mutation and crossover were used for new model (child) generation. Arithmetic crossover operation requires two parents (models **m1** and **m2**) to create two children **y1** and **y2**:

$$y1 = \alpha.\boldsymbol{m1} + (1-\alpha).\boldsymbol{m2}$$
$$y2 = \alpha.\boldsymbol{m2} + (1-\alpha).\boldsymbol{m1} \qquad (15)$$

If $\alpha = 1$, then **y1** = **m1** and **y2** = **m2**. Also, if $\alpha = 0$, then **y1** = **m2** and **y2** = **m1.** Thus, by assigning a value to α from the range (0, 1), new models will inherit their values from either **m1** or **m2**. Generally, a small value of δ is considered for creation of some random divergent models from the convex formation defined above. Depending on how large the δ value is, these minor divergent answers will increase the exploitation or sometimes exploration efficiency of the algorithm:

$$\alpha = random(-\delta, 1+\delta) \qquad (16)$$

For a model **m1**, mutated solution is:

$$\boldsymbol{y1} = \boldsymbol{m1} + \beta \qquad (17)$$

where the parameter β is a random percentage of maximum mutation step defined by the operator:

$$\boldsymbol{\beta} = r * (\max mutation\ step\ (in\ meter))\ ;\ r = random(-1,1) \qquad (18)$$

2-8 Parent selection tournaments

The parent selection process for genetic operations is also important. Among the objective functions, the gravity data fitness is more important than the regularization function. Considering this point, we used a binary tournament selection method (Miller and Goldberg, 1995) to find possible candidates in crossover operation and a roulette wheel selection method (Blickle and Thiele, 1996) to find possible candidates for mutations. The binary tournament method uses the total fitness for parent selection, while the roulette wheel method utilizes a probability distribution function pertaining to gravity objective function. Lower gravity RMSE values are more likely to be selected as parents. These selection modes lead the algorithm to better exploitation (since the mutation process takes place among the models with lower RMSE values) and a good exploration (by a random selection of fitter solutions and using them in crossover operation) of the solution space.

2-9 Random local mutation

It is important to consider that by using the multi-objective method, we increase the dimension of the solution space. We are not exploring and minimizing an array of gravity data, but a plane of gravity and depth data. On the other hand, the number of parameters in the problem is usually high, and the problem has non-unique solutions. Thus, it does not seem to be efficient enough only using general genetic operations in the multi-objective algorithm, hence the need to add some features in genetic operations in order to increase the efficiency of the algorithm.

In the each iteration, two mutation operations are applied in the algorithm. The first one is random local dual side dynamic mutation defined as following:

$$\boldsymbol{y1}(\boldsymbol{i},\boldsymbol{j}) = \boldsymbol{m}(\boldsymbol{i},\boldsymbol{j}) + \beta_{dyn}$$
$$\boldsymbol{y2}(\boldsymbol{i},\boldsymbol{j}) = \boldsymbol{m}(\boldsymbol{i},\boldsymbol{j}) - \beta_{dyn} \quad (19)$$

The first noticeable point is that two children are created. The term $\boldsymbol{m}(\boldsymbol{i},\boldsymbol{j})$ means that the mutation process takes place only on a random range of depth parameters (from the point $\mathbf{i}$ to the point $\mathbf{j}$) in model $\boldsymbol{m}$. In addition, we use a dynamic value for mutation here, which decreases by a fixed rate during optimization process.

2-10 Guided mutation

Sometimes, after a large number of iterations, being trapped into a local minimum very close to acceptable global optimal solutions, the algorithm will not show further progress. The first idea for covering such unwilling problems is to increase the number of populations, but it is not efficient at all. On the other hand, in gravity problems, after applying Bouguer correction, the maximum gravity effect for every piece of an anomaly would take place right above the structure. We use this information as a guided mutation strategy in producing new solutions by considering mutation only in areas where a considerable data misfit is detected. This operation will exploit some already optimized answers.

$$\boldsymbol{y}_{\boldsymbol{guided}}(\boldsymbol{i},\boldsymbol{j}) = \boldsymbol{m}(\boldsymbol{i},\boldsymbol{j}) + \beta_{dyn}\ ,\ in\ range\ (\boldsymbol{i}\ ,\boldsymbol{j})\ where\ |\Delta\boldsymbol{g}| > mean(|\Delta\boldsymbol{g}|) \quad (20)$$

After all, the solutions created in this section will take part alongside archive solutions in the next assessments of iteration.

The parameters crossover (δ) and mutation (β_{dyn}) in the genetic algorithm are the main variables controlling the trend of the algorithm. While being dimensionless, these parameters are sensible as they are defined in the form of a percentage of the search space. Larger values for parameters δ and β_{dyn} give rise to more diverse solutions and a better exploration, while smaller values for these parameters lead to more focused solutions and better exploitation.

3 Evaluation

3-1 Synthetic models

A synthetic model for a sedimentary layer with homogenous density contrast of -600 kg/m^3 is created (Fig. 3). Maximum depth of 8 km is considered for this model. Having almost 6 km change in layer depth in different locations, makes this model a suitable test case for efficiency of the algorithm. We tested the algorithm for this model with parameters recorded in Table 1. The RMSE value for the solutions changes from 0.534 mGal for the best solution, to 16.854 mGal for the weakest model. Fig. 4 shows the Pareto-front created by the algorithm and Fig. 5 describes the error distribution of depth values from the synthetic model for 10 models with lowest RMSE values. Fig. 6 shows the result of algorithm for the synthetic model. RMSE value for plotted model is 0.534 mGal.

To evaluate the stability of the algorithm in presence of high level of noise, a heavy white Gaussian noise with maximum amplitude of 2.6 mGal and average amplitude of 0.89 mGal added to previous model. It is important to consider that such an extreme noise on a dataset is not practical, but it is implemented here to evaluate stability of the suggested method. Figs. 7 and 8 demonstrate two of the results of the algorithm in presence of heavy noise. These answers are chosen among one hundred possible solutions suggested by the method. One of them (Fig. 7) has the lowest RMSE value for gravity data while the other (Fig. 8) has a suitable smoothness among the answers. All parameters are chosen according to the Table 1. Because of applying the smoothing term as a separate cost function in the algorithm, even in the presence of a high level of noise, stable solutions are acquired.

For more evaluation, we decided to add more details to the synthetic model by changing the geometry of the layer. Saving the previous amount of white noise in the gravity output, we added another local minimum to the geometry of layer. In addition, some harsh steeps are added to the layer to assess the steadiness of the method in presence of considerable sudden changes in depth values. The output is presented in Fig. 9.

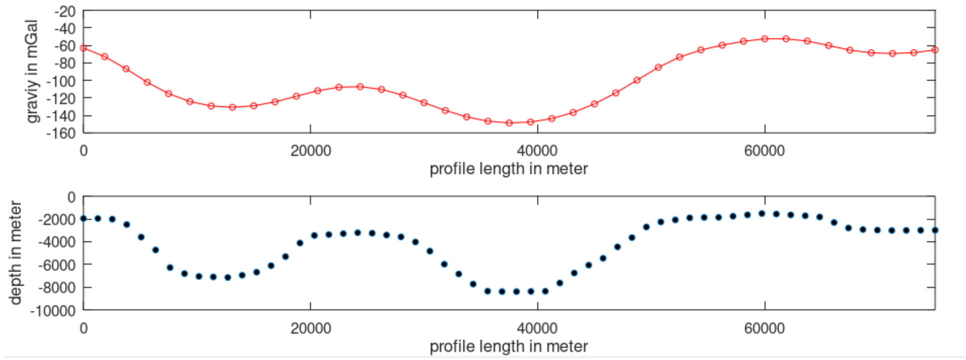

Fig 3. Substructure geometry and gravity effect of a synthetic layer on the ground. Due to a homogenous density contrast, the values of gravity field change with geometry of the layer.

Table 1. Parameter values applied in inversion of synthetic data.

Parameters	Values
Density contrast for layer	-600 kg/m^3
Maximum depth for search space	10000 (meter)
Minimum depth for search space	0 (meter)
Population size	200
Archive size	100
Maximum iteration	200
Percentage of mutated solutions	10%
Percentage of crossed solutions	90%
Crossover parameter (δ)	0.05
Mutation parameter (β)	0.05

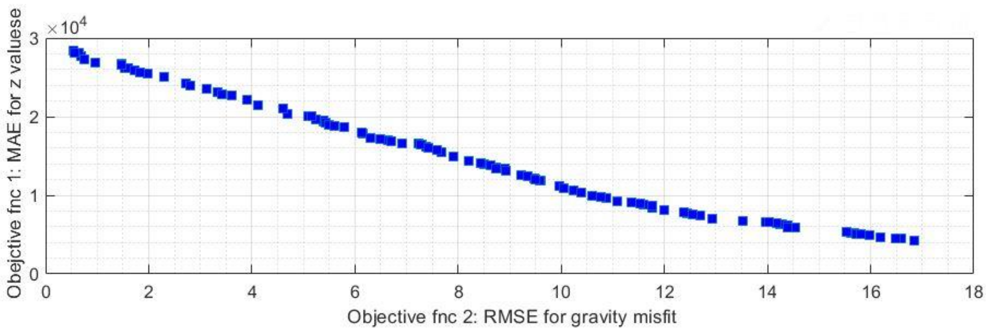

Fig 4. Pareto front for synthetic data modelling. The population of Pareto front is 100 solutions (full archive). These models are the most non-dominated solutions found by algorithm. Their gravity RMSE varies from 0.5 to 17 mGal.

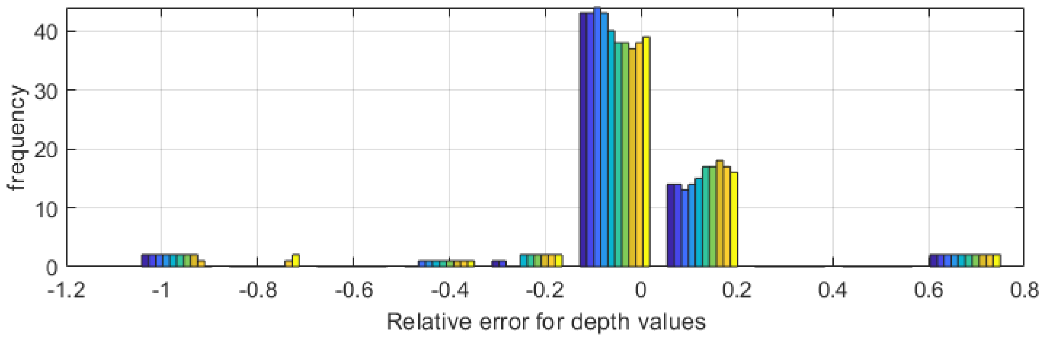

Fig 5. Relative error distribution for 10 solutions with the lowest RMSE values. Generally, a Gaussian distribution for errors is expected. The sharper is the bell shape distribution. The lower values are the errors.

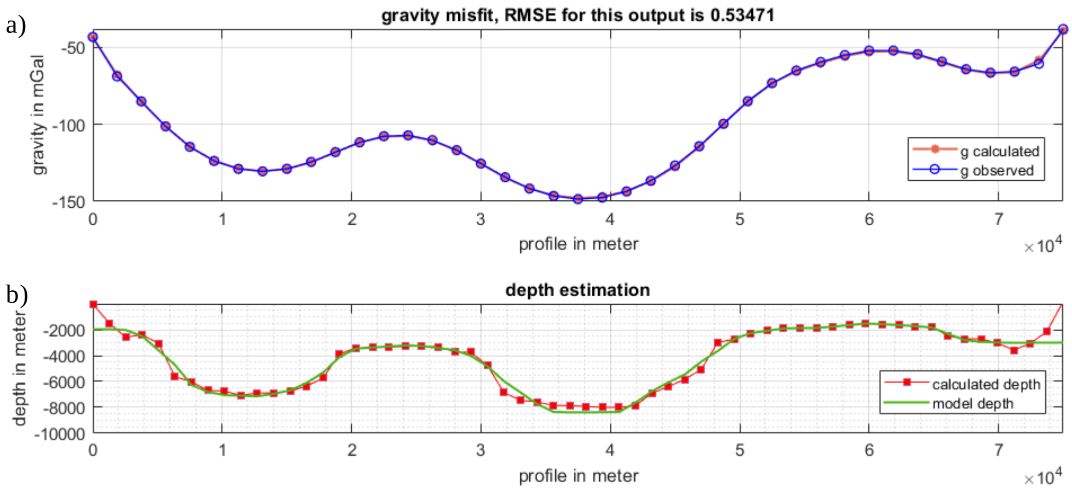

Fig 6. One of the solutions of the algorithm and its gravity effect. (a) Gravity effect of synthetic model (observed) vs. gravity effect of algorithm model (calculated). (b) Green line is boundary of layer from the synthetic model. The red line is the calculated depth.

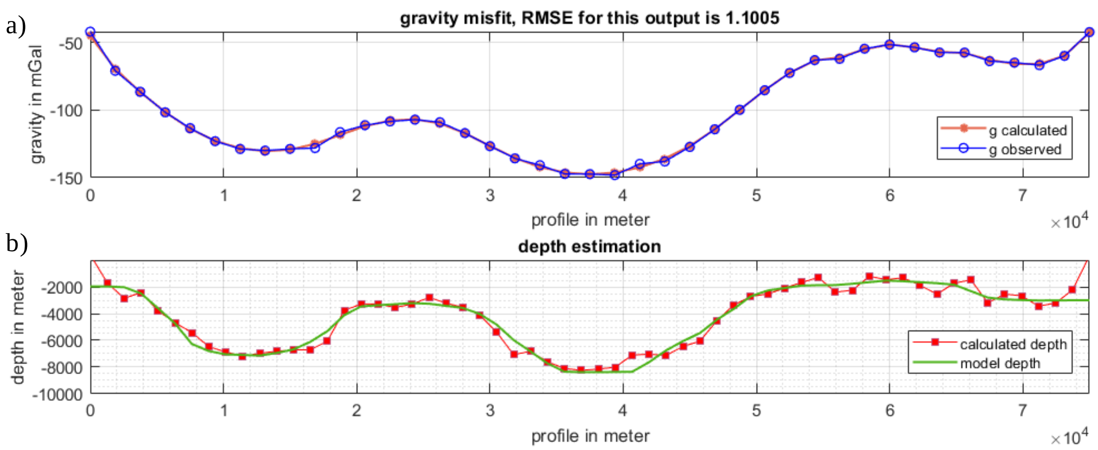

Fig 7. One of the suggested solutions for noisy data modelling. This solution has the lowest RMSE value among the answers. For all the solutions, RMSE values increased in comparison to previous model, but they are still acceptable and the model is valid.

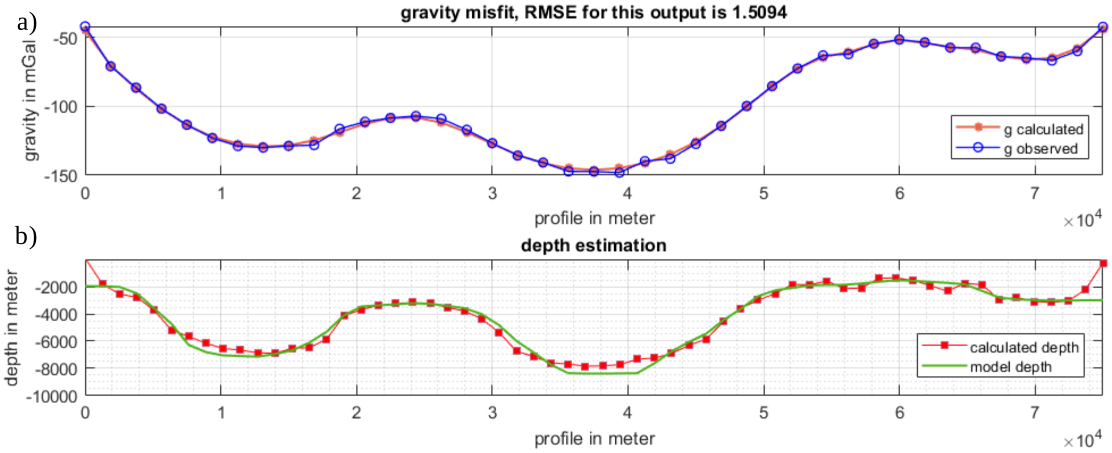

Fig 8. Another solution for noisy data modelling. This solution lacks in favorable RMSE value, but it seems to have a suitable smoothness. For all the solutions, RMSE values increased in comparison to previous model, but they are still acceptable and the model is valid.

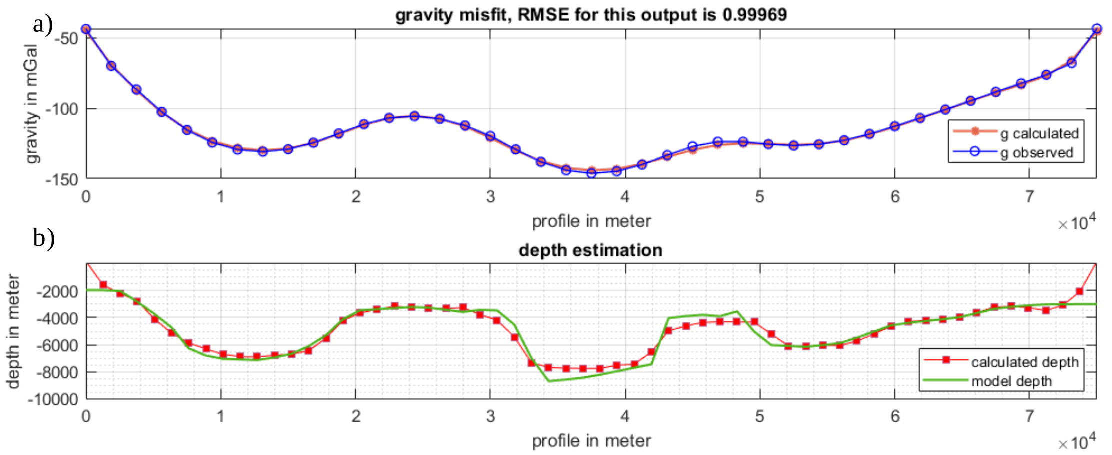

Fig 9. Synthetic model with sharper steeps and rugged structure. Although this model is more complicated but the RMSE value for gravity misfit is lower than previous model due to stochastic nature of search method.

3-2 Analysis on real data

As a practical application of this algorithm, the gravity data from Recôncavo basin in Brazil is considered for depth to basement calculations. Gravity anomaly in the area mainly occurs because of the basement relief in the area (Le˜ao et al., 1996). Fig. 8 shows the Bouguer anomaly map of basin in northeast Brazil (Silva et al., 2006). A homogenous density contrast of 260 kg/m^3 is considered for data modelling (Barbosa et al., 1997 and 1999; Le˜ao et al., 1996; Silva et al., 2006). Silva et al. (2006) described the geology of the area and used the profile A-A′ for further studies. We use the same profile (using digitized data) to compare our results with previous studies. Fig. 9 shows the inversion result and also previous studies. Fig. 10 illustrates the Pareto front created for solving this problem.

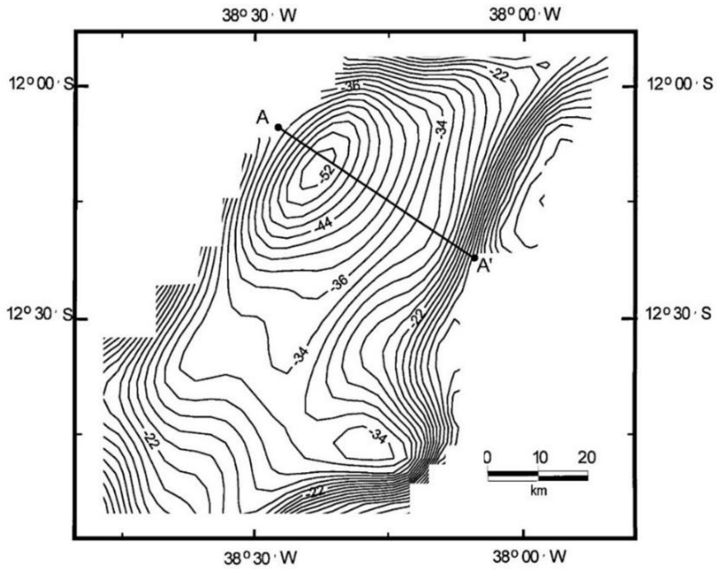

Fig 10. Bouguer map of Recôncavo basin (Brazil). Profile A-A' is considered for gravity modelling (modified after Silva et al. (2006)).

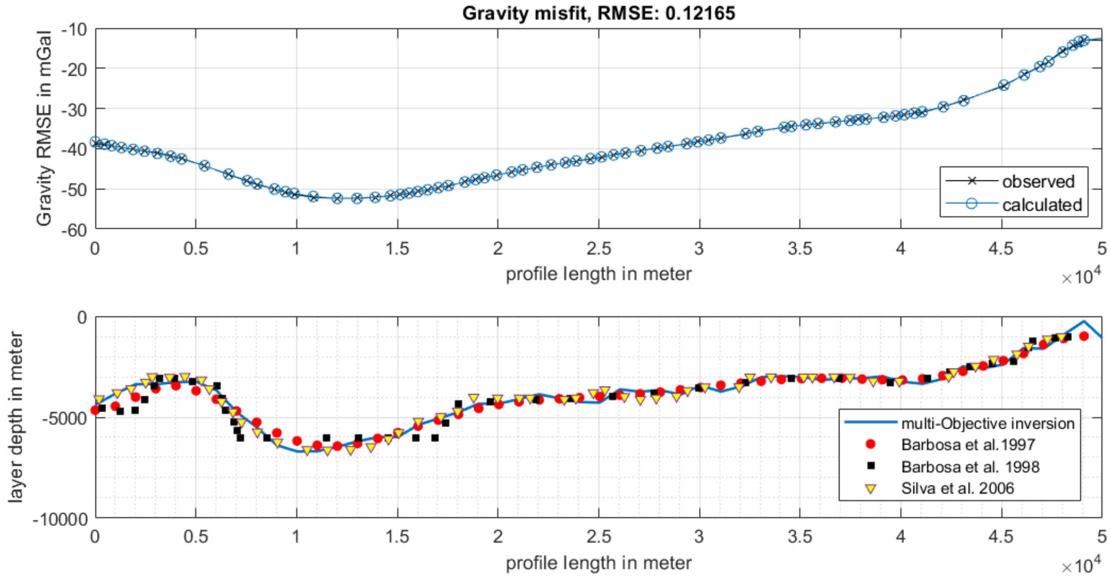

Fig 11. Data modelling results for multi-objective method and previous studies. Upper diagram shows the data misfit between multi-objective solution and observed data. Lower diagram illustrates basement relief in A-A' profile according to different methods.

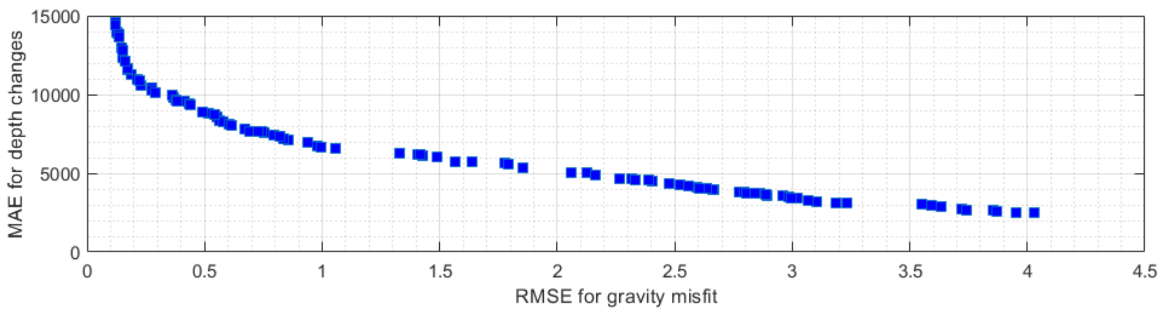

Fig 12. Pareto front for real data modelling in Recôncavo basin (Brazil). A good convergence for RMSE gravity is achieved on the upper left corner of the figure.

Table 2. Parameter values applied in inversion of real data.

Parameters	Values
Density contrast	-260 kg/m^3
Minimum depth in search space	0 meter
Maximum depth in search space	10000
Population size	300
Archive size	150
Maximum iteration	400
Percentage of mutated solutions	10%
Percentage of crossed solutions	90%
Crossover parameter (δ)	0.05
Mutation parameter (β)	0.05

Table 3. Relative errors of depth values between multi-objective algorithm and other methods.

Method	Relative error
Barbosa et al. (1997)	0.1351
Barbosa et al. (1999)	0.1494
Silva et al. (2006)	0.1159
multi-objective method	0.12

Parameters used in this process are presented in Table 2. The final RMSE value in our data modelling method is 0.12 mGal, which means that the algorithm works properly. All previously suggested models are accepted due to different geological interpretations available for the area (Silva et al., 2006). Here, to exhibit the similarity between these models and the results of this method, mean absolute relative errors for depth values are calculated and the outputs are shown in Table 3. The model proposed by multi-objective method is the most identical (lowest relative error) to the model presented by Silva et al. (2006).

4 Conclusion

To solve the gravity data inversion problem, a 2D gravity data modelling method based on a multi-objective algorithm is presented. The method does not need to directly deal with the inverse formulations due to the implementation of the genetic algorithm as an iteratively forward optimization technique. Furthermore, this method does not require a weighted regularization coefficient; thus, the time for finding a weighting matrix and parameter of the regularization term will be saved and will be spent on model searching instead. Moreover, as a global optimization method, it solves the inversion problem without any specific initial model. All these improvements make this method a fast and considerably effective for the case of layer boundary determination. We specifically applied this method to determine a two-dimensional layer boundary. The efficiency and validity of this method are tested with a synthetic model. For further evaluation of the stability of this algorithm, noisy synthetic data is used and it is proved that this method shows a great convergence even in the presence of noise. All the results are demonstrated using different tables and diagrams. As a practical example of this method, a basement relief in Brazil was modelled. The results are in complete conformity with previously done researches.

References

Akca., I., Gunther, T., Muller-Petke, M., Basokur, A. T., Yaramanci, U., 2014, Joint parameter estimation from magnetic resonance and vertical electric soundings using a multi-objective genetic algorithm: Geophysical Prospecting, **62**, 364–376.

Barbosa, V. C. F., Silva, J. B. C., and Medeiros, W. E., 1997, Gravity inversion of basement relief using approximate equality constraints on depths: Geophysics, **62**, 1745–1757.

Barbosa, V. C. F., Silva, J. B. C., and Medeiros, W. E., 1999, Gravity inversion of a discontinuous relief stabilized by weighted smoothness constraints on depth: Geophysics, **64**(5), 1429-1437.

Blickle, T., and Thiele, L., 1996, A comparison of selection schemes used in evolutionary algorithms: Evolutionary Computation, **4**(4), 361–394.

Coello, C. A. C., 1999, A comprehensive survey of evolutionary-based multiobjective optimization techniques: Knowledge and Information Systems, **1**(3), 269-308.

Golub, G. H., Heath, M., and Wahba, G., 1979, Generalized cross validation as a method for choosing a good ridge parameter: Technometrics, **21**, 215–23.

Hansen, P. C., 1992, Analysis of discrete ill-posed problems by means of the L-curve: SIAM Review.

Hubert, M. K. A., 1948, A line-integral method for computing the gravimetric effect of two-dimensional masses: Geophysics, **13**, 215–222.

Lawrence, K. P., and Phillips, R. J., 2003, Gravity/topography admittance inversion on Venus using niching genetic algorithms: Geophys. Res. Lett., **30**(19), 1994.

Le˜ao, J. W. D., Menezes, P. T. L., Beltr˜ao, J. F., and Silva, J. B. C., 1996, Gravity inversion of basement relief constrained by the knowledge of depth at isolated points: Geophysics, **61**, 1702–1714.

Li, Y., and Oldenburg, D. W., 1999, 3D Inversion of DC resistivity data using an L-curve criterion: 69th Annual International Meeting., Society of Exploration Geophysicists, Expanded Abstracts, 251–254.

Miernik, K., Bogacz, A., Kozubal, A., Danek, T., and Wojdyla, M., 2016, Pareto joint inversion of 2D magnetotelluric and gravity data – towards practical applications: Acta Geophysica, **64**(5), 1655–1672.

Miller, B. L., and Golberg, D. E, 1995, Genetic algorithms tournament selection and the effects of noise: Complex Systems, **9**(3), 193-212.

Montesinos, F. G., Arnoso, J., and Vieira, R., 2005. Using a genetic algorithm for 3-D inversion of gravity data in Fuerteventura (Canary Islands): International Journal of Earth Sciences: **94**, 301–316.

Morozov, V. A., 1966, On the solution of functional equations by the method of regularization: Soviet Mathematics Doklady, **7**, 414–417.

Silva, J. B. C., Costa, D. C. L., and Barbosa, V. C. F., 2006, Gravity inversion of basement relief and estimation of density contrast variation with depth: Geophysics, **71**, J51–J58.

Silverman, B. W., 1986, Density estimation for statistics and data analysis: Chapman and Hall.

Telford, W. M., Geldart, L. P., and Sheriff, R. E., 1990, Applied Geophysics: Cambridge University Press.

Talwani, M., Worzel, J. L., and Landisman, M., 1959, Rapid gravity computations for two-dimensional bodies with application to the Mendocino submarine fracture zone: J. . Geophys. Res., **64**, 49-59.

Zhang, J., Wang, C., Shi, Y., Cai, Y., Chi, W., Dreger, D., Cheng, W., and Yuan, Y., 2004, Three-dimensional crustal structure in central Taiwan from gravity inversion with a parallel genetic algorithm: Geophysics, **69**, 917–924, DOI:10.1190/1.1778235.

Zitzler, E., Laumanns, M., and Thiele, L., 2001, SPEA2: Improving the Strength

Pareto Evolutionary Algorithm: TIK-Report, 103.

Zitzler, E., and Thiele, L., 1999, Multi-objective evolutionary algorithms: A comparative case study and the strength Pareto approach: IEEE Transactions on Evolutionary Computation, **3**(4), 257–271.